Characterization of Fast Pyrolysis Products Generated from Several Western USA Woody Species

Jacqueline M. Jarvis,[†] Deborah S. Page-Dumroese,*[‡] Nathaniel M. Anderson,[§] Yuri Corilo,[†] and Ryan P. Rodgers[†]

[†]National High Magnetic Field Laboratory, Florida State University, 1800 East Paul Dirac Drive, Tallahassee, Florida 32310, United States

[‡]U.S. Department of Agriculture, Forest Service, Rocky Mountain Research Station, 1221 S. Main, Moscow, Idaho 83843, United States

[§]U.S. Department of Agriculture, Forest Service, 200 East Broadway, Missoula, Montana 59802, United States

Ⓢ Supporting Information

ABSTRACT: Woody biomass has the potential to be utilized at an alternative fuel source through its pyrolytic conversion. Here, fast pyrolysis bio-oils derived from several western USA woody species are characterized by negative-ion electrospray ionization Fourier transform ion cyclotron resonance mass spectrometry (ESI FT-ICR MS) to determine molecular-level composition. The composition and properties (pH, electrical conductivity, and elemental analyses) of the biochar byproduct were also determined. The bio-oils are comprised mainly of Ox species. Oak (*Quercus garryana* Douglas ex Hook), mixed conifer (*Pseudotsuga menziesii* Mirb. Franco, *Tsuga heterophylla* (Raf.) Sarg, *Abies concolor* (Gord. & Glend.) Lindl. ex Hildebr.), and scotch broom (*Cytisus scoparius* (L.) Link) bio-oils contain lower O_x (O_1–O_7) species that exhibit bimodal distributions whereas mixed conifer feedstock from a fire salvage harvest contains a larger range of Ox species (O_2–O_{13}) that exhibit a mainly monomodal distribution. Boron-containing species in the pyrolysis oils were also identified for the first time by FT-ICR MS. Biochar analysis revealed that all biochars had similar pH values (~7−8); however, the electrical conductivity and elemental analyses varied across the samples. Understanding the composition of pyrolysis byproducts will help direct their uses to the most appropriate locations.

■ INTRODUCTION

Significant areas of the western USA face land management challenges related to wildfire, insect and disease outbreaks, and invasive species. In addition, the cost of biomass removal often exceeds its value, despite increasing interest in forest biomass utilization.[1] There are few markets for residual biomass, but woody biomass could become a sustainable substitute for fossil fuels. It is estimated that more than 11 million hectares of forestlands could benefit from hazardous fuel reduction treatments, yielding approximately 310 million oven dry Megagrams for bioenergy production.[2]

Fast-pyrolysis technologies to convert woody biomass to bio-oil and biochar are becoming more common[3] and may be an approach to both profitable and sustainable forest biomass utilization. Many pyrolysis units are relatively small and can be located near biomass harvest areas, thereby reducing transportation costs associated with moving bulk biomass to a processing plant. The transportable fuel (bio-oil) can then be transported efficiently and used for heat, power, and chemical production.[4] Additionally, pyrolysis units produce a charcoal byproduct (biochar) that can have a market value of its own but might be primarily used for carbon sequestration. As of 2006, approximately 97% of all transportation energy used in the United States was derived from nonrenewable petroleum and more than half of this oil was from nondomestic sources.[5] The use of forest biomass for energy provides significant environmental advantages such as reduction of greenhouse gas emissions.[6]

Unfortunately, there is little known about specific biochar properties and the molecular-level composition of bio-oil. Thus, prior to large-scale use of bio-oil or biochar, we must understand the basic characteristics of bio-oil and its byproducts to avoid potential negative impacts. Our objectives are to determine the composition of bio-oil and characterize the biochar produced from a range of forest species considered viable for pyrolysis.

Oasmaa et al. have performed extensive studies on fast pyrolysis bio-oils derived from forestry residues and separated bio-oil components into larger compounds classes.[7−10] The typical compounds include aldehydes, ketones, sugars (carbohydrates), extractives (fatty and resin acids), and lignin (methoxyphenols).[7−10] Since then, high-resolution mass spectral characterizations of bio-oils have been conducted by several groups to gain a molecular-level understanding of bio-oil composition.[11−17] Negative-ion electrospray ionization has been the method of choice for the analysis of bio-oils because the most abundant species within bio-oil, O_x species derived from the decomposition of cellulose, hemicellulose, and lignin,[8] are easily deprotonated to form ions. Positive-ion electrospray ionization (ESI) analysis of bio-oils is typically not conducted because of the likelihood of adduct formation, thus increasing the complexity of the samples without significant gains in

compositional information (i.e., sodium will adduct to O_x species that are ionized by (−) ESI). However, positive-ion ESI can provide beneficial analysis of samples with high nitrogen contents,[14] in which the basic N_x and N_xO_y species are more efficiently ionized than sodium adducts. Other ionization techniques have been used to analyze bio-oils, such as APPI, APCI, and DART, to target both nonpolar and polar species with success.[16−18] For this study, we will focus on negative-ion ESI to target the acidic, polar species within the bio-oil samples within the 160−1000 Da range.

■ METHODS

Pyrolysis Conditions and Feedstock. The biochar and bio-oil characterized in this study were produced using a mobile, pilot-scale 1 dry ton per day (dtpd) fast pyrolysis reactor manufactured by Abri Tech, Incorporated, Namur, QC (formerly Advanced Biorefinery, Incorporated, Ottawa, ON) and operated by Biochar Products, Halfway, OR. This reactor uses an externally heated hot shell auger with an inert high density 2.0 mm steel heat carrier. The carrier is mixed with the feedstock in the main auger and then separated from the biochar using a rotary trommel screen. No carrier gas is required. Total residence time in the system is 5 to 7 min, with carbonization and evacuation of gas phase volatiles occurring in the main auger in 2 to 4 s. Fine-grained biochar suspended in process gas is separated in a gas cyclone prior to the gases entering the condensation system, and all biochar exits the reactor though a continuous feed, liquid cooled output auger. Operating temperature for both the main auger and carrier reservoir is 400 °C and ranged from 388 and 447 °C during production cycles. Yields for dry wood feedstocks processed with this system have been reported to be 15% process gas, 60% bio-oil, and 25% biochar by weight,[7] and observed biochar production was 5 to 10 kg hr^{-1}, depending on operating conditions. The pyrolysis unit is paired with a propane/process gas-fired chain flail dryer that simultaneously dries and pulverizes feedstock before pyrolysis. All feedstocks were processed with this dryer prior to pyrolysis.

This system was used to produce biochar and bio-oil from five lignocellulosic feedstocks, including four tree species and one exotic invasive woody shrub (Table 1). All of these feedstocks were harvested in western Oregon. Both the mixed species and single species feedstocks used in this study are representative of forest treatment residues (slash from thinning operations, forest health harvests, or wildfire salvage materials) typically produced in this region. Woody materials less than 6 in. in diameter, including stem, crown, bark, and foliage, were processed with conventional horizontal grinders to an average particle size of 1.9 cm or smaller. Ground material was stored in one ton batches in polypropylene bulk bags for four to seven months prior to pyrolysis, with two exceptions. Mixed conifer beetle kill salvage was stored in bulk bags for 7 days prior to pyrolysis, and lodgepole pine was stored outdoors near the harvest site for 20 months prior to pyrolysis. All feedstocks were pulverized to an average particle size of 0.4 cm and dried to <10% water content prior to processing. The water content of feedstocks immediately prior to drying ranged from 18% to 24%. Time between harvest or fire and grinding ranged from 1 week (mixed conifer) to 6 years (mixed conifer beetle killed salvage), but most feedstocks were cut, ground, and converted to biochar over a one year period. Biochar production took place between December 16, 2009, and May 16, 2010.

Biochar Chemical Analyses. The determination of total carbon (C) and total nitrogen (N) for both feedstock and biochar was by dry combustion on a TruSpec CN analyzer (Leco Corporation, St. Joseph, MI). Samples were dried and homogenized prior to analysis; feedstocks were ground to pass through a 420 μm screen, and char was ground to a fine powder. Sample size and analysis method reflected the unique composition of the samples; feedstocks were treated as organic material while the biochar was analyzed using soil (mineral) methods (higher oxygen flow during the burn phase to ensure complete combustion of the material). The TruSpec CN uses

Table 1. Feedstocks Used to Produce the Biochar and Bio-Oil Characterized in This Study[a]

description	year cut or burned	species	species mix
mixed conifer	2009	*Pseudotsuga menziesii* Mirb. Franco	70
		Tsuga heterophylla (Raf.) Sarg.	20
		Abies concolor (Gord. & Glend.) Lindl. Ex Hildebr.	10
mixed conifer, fire salvage	2010	*Pseudotsuga menziesii*	60
		Tsuga heterophylla	30
		Abies concolor	10
mixed conifer, beetle kill salvage	2003	*Pseudotsuga menziesii*	40
		Tsuga mertensiana (Bong.) Carrière	10
		Abies concolor	10
		Pinus contorta Douglas ex Loudon	40
Oregon white oak	2008	*Quercus garryana* Douglas ex Hook	100
scotch broom (invasive shrub)	2009	*Cytisus scoparius* (L.) Link	100

[a]Production took place between December 16, 2009, and May 16, 2010.

an infrared (IR) detector to measure carbon and a thermal conductivity (TC) cell to determine N.[19]

An unconsolidated biochar sample was used to assess sample pH. A char/distilled water solution with a 1:4 ratio was made, and pH was determined with an Orion 4-Star meter and electrode (Thermo Scientific, Beverly, MA). Electrical conductivity (EC) of each sample was conducted on the same equipment as pH. Carbon, N, EC, and pH analyses were conducted at the Rocky Mountain Research Station, Moscow, ID. The biochar was also analyzed for potassium (K) and phosphorus (P),[20−22] exchangeable calcium (Ca), magnesium (Mg), sulfur (S), chromium (Cr), copper (C), iron (FE), manganese (Mn), and zinc (Zn).[23,24] Chemical property analyses were conducted at the Analytical Sciences Laboratory, University of Idaho, Moscow, ID.

Bio-Oil Sample Preparation. Stock solutions were prepared at a concentration of 1 mg/mL in methanol (HPLC grade, JT Baker (Phillipsburg, NJ) or Sigma-Aldrich (St. Louis, MO)). Final samples were further diluted in methanol to 500 μg/mL, and 1% (v/v) ammonium hydroxide solution (28% in water, Sigma-Aldrich, St. Louis, MO) was added to aid in deprotonation prior to negative-ion ESI Fourier transform ion cyclotron resonance mass spectrometry (FT-ICR MS) analysis. A syringe pump (0.5 μL/min) delivered the samples to the ionization source.

Mass Spectrometry. Samples were analyzed with a custom-built 9.4 T Fourier transform ion cyclotron resonance mass spectrometer.[25] Data collection was facilitated by a modular ICR data acquisition system (PREDATOR).[26,27] External calibration of the instrument is performed biweekly by use of an ESI tuning mix (Agilent, Santa Clara, CA) to correct for temporal drift of the magnetic field. Negative ions generated at atmospheric pressure were introduced into the mass spectrometer via a heated metal capillary. Ions were guided through the skimmer region (∼2 Torr) and allowed to accumulate in the first octopole (rf-only).[28] Ions were sent through the quadrupole (mass transfer mode) to a second octopole where the ions were collisionally cooled for 1 ms with helium gas (∼(4−5) × 10^{-6} Torr at gauge) before passage through a transfer octopole to the ICR cell[29] (open cylindrical Penning trap). Octopole ion guides were operated at 2.0 MHz and 240 V$_{P-P}$ rf amplitude.

Multiple (100) individual time-domain transients were coadded, Hanning-apodized, zero-filled, and fast Fourier transformed prior to frequency conversion to mass-to-charge ratio[30] to obtain the final mass spectrum. Transient length was ~4.6 s. All observed ions were singly charged, as evident from unit m/z spacing between species which differ by $^{12}C_c$ vs $^{13}C_1{}^{12}C_{c-1}$.

Data Analysis and Visualization. Data were analyzed, and peak lists were generated with custom-built software (MIDAS).[15] Internal calibration of the spectrum was based on a homologous series whose elemental compositions differ by integer multiples of 14.01565 Da (i.e., CH_2).[31]

Compounds with the same heteroatom content (i.e., same n, o, and s in $C_cH_hN_nO_oS_s$) but differing in degree of alkylation may then be grouped together in a spreadsheet.[32] Because a single homologous series does not typically span the entire mass range for a bio-oil sample, multiple homologous series (various O_x species) were needed to achieve broadband internal calibration.

Data are visualized by relative abundance histograms for heteroatom classes greater than 1% relative abundance and from isoabundance-contoured plots of double bond equivalents (DBE = number of rings plus double bonds to carbon) vs carbon number for members of a single heteroatom class. The relative abundance scale in isoabundance-contoured plots is scaled relative to the most abundant species in that class.

■ RESULTS AND DISCUSSION

Oak, Mixed Conifer, and Scotch Broom Bio-Oils. Figure 1 shows the heteroatom classes identified at >1% relative
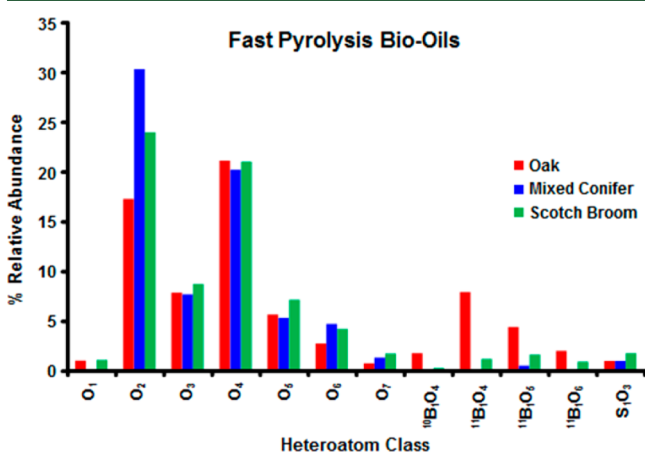
Figure 1. Heteroatom class distribution for the oak (red), mixed conifer (blue), and scotch broom (green) bio-oils derived from (−) ESI 9.4 T FT-ICR mass spectra. Heteroatom classes with greater than 1% relative abundance in any sample are shown.

abundance in oak, mixed conifer, and scotch broom bio-oils derived from negative-ion ESI FT-ICR MS. All three bio-oils contain a similar class composition of the O_x species, ranging from O_1 to O_7. These bio-oils contain fewer oxygen atoms than previously characterized bio-oils[11] as well as the other bio-oils discussed in this paper (discussed later). The relative abundances of the common O_x classes are also similar except for the O_2 class in which the mixed conifer bio-oil has ~6% and ~13% higher relative abundance than scotch broom and oak bio-oils. Differences in the O_2 class relative abundances are most likely due to differing amounts/types of extractives (fatty acids and resin acids) in each bio-oil. The S_1O_3 species most likely correspond to linear alkylbenzenesulfonates (detergents) that were unwantedly introduced into the sample prior to analysis. Exhaustive cleaning of vials and associated sample preparation equipment did not reduce contamination. Thus,

the contamination most likely occurred in the oil collection process.

The oak and scotch broom bio-oils also contain B_1O_x species in >1% relative abundance (Figure 1). The most abundant B_1O_x species are those containing 4 and 5 oxygen atoms per boron found in both the oak and scotch broom bio-oils. All three bio-oils also contain additional B_1O_x species not represented on the class graph because they are present in >1% relative abundance (Table S1, Supporting Information). Boron has two stable isotopes of relatively high natural abundance, ^{10}B at 20% and ^{11}B at 80%, which helps to confirm elemental assignments of boron. The more abundant $^{11}B_1O_x$ classes ($^{11}B_1O_4$ and $^{11}B_1O_5$) in oak have the corresponding $^{10}B_1O_x$ classes at ~20% the abundance of the monoisotopic class to validate their assignment. To further validate the assignment of boron-containing species in oak, the isoabundance-contoured plots of DBE vs carbon number for the B_1O_4 and B_1O_5 classes (Figure 2) show that the $^{10}B_1O_x$ classes cover
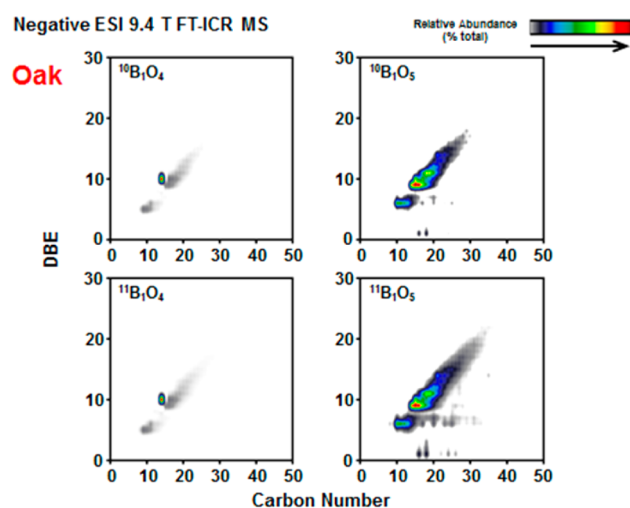
Figure 2. Negative-ion ESI 9.4 T FT-ICR MS isoabundance-contoured plots of double bond equivalents (DBE) vs number of carbons for $^{10}B_1O_4$-$^{10}B_1O_5$ (top) and $^{11}B_1O_4$-$^{11}B_1O_5$ (bottom) classes in oak bio-oil. Similar compositional space coverage for both boron isotopes verifies peak assignment.

the same compositional (C# and DBE) space as the $^{11}B_1O_x$ classes except for the loss of some of the lower abundant compounds in the $^{10}B_1O_x$ plots.

Boron was determined to be an essential element in the development of plants.[33−38] Since then, naturally occurring boron-containing compounds have been identified in plants.[39−41] Characterization by ^{11}B-NMR has shown that boron in boron-polysaccharides exist as a tetravalent 1:2 borate-diol complex.[42] Boron polyol complexes have also been isolated and characterized by MALDI-FTMS.[43] These findings correlate with our FT-ICR MS data in which boron atoms are only seen in compounds containing at least 4 oxygen atoms, which supports tetravalent borate complexes. Figure 3 shows oak, mixed conifer, and scotch broom bio-oils negative-ion ESI isoabundance-contoured plots of DBE vs carbon number for various O_x heteroatom classes.

The O_2 class in all bio-oils is dominated by C_{12}–C_{30} saturated fatty acids at DBE 1. The most abundant O_2 compounds in the oak and scotch broom bio-oils most likely correspond to the fatty acids palmitic and steric acid whereas
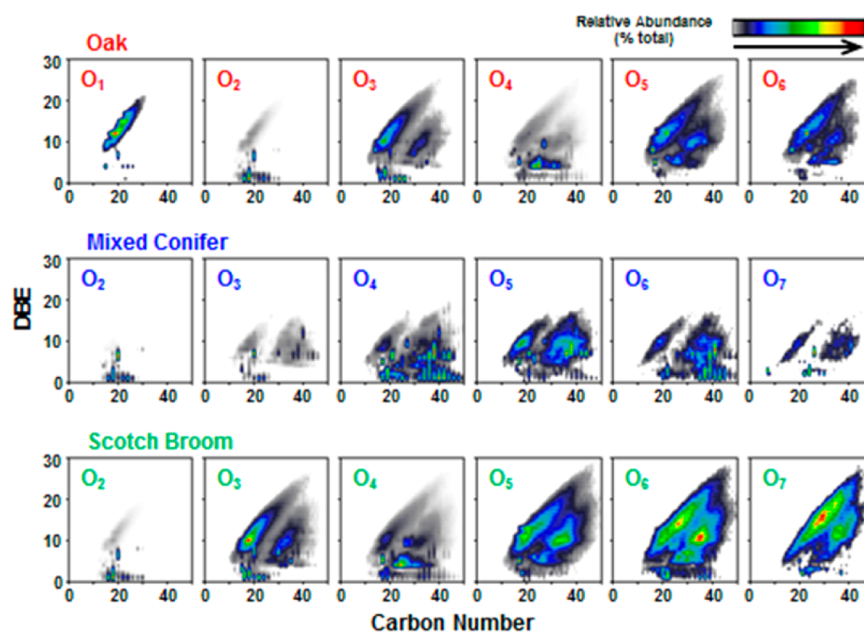
Figure 3. Negative-ion ESI 9.4 T FT-ICR MS isoabundance-contoured plots of double bond equivalent (DBE) vs carbon number plots for the various O_x classes from oak (red, top), mixed conifer (blue, middle), and scotch broom (green, bottom) bio-oils. Multimodal compositional distributions are observed in classes containing >2 oxygens.

the most abundant compounds in the mixed conifer bio-oil which possibly correspond to resin acids at C_{20} and DBE 6−7 (abietic acid, dihydroabetic acid, and/or isomers). Mixed conifer bio-oil appears to consist of diacids of low DBE and carbon numbers >30 in high abundance. O_x classes in all bio-oils have multimodal distributions when the oxygen number is >2. The multimodal distributions along with the similar slopes of all the O_x plots points to polymeric addition.

Mixed Conifer Salvage Bio-Oils. Figure 4 shows the heteroatom classes identified at >1% relative abundance in the mixed conifer salvage bio-oils derived from negative-ion ESI FT-ICR MS. Both mixed conifer salvage bio-oils contain O_x species that range from O_2 to O_{13} with similar relative
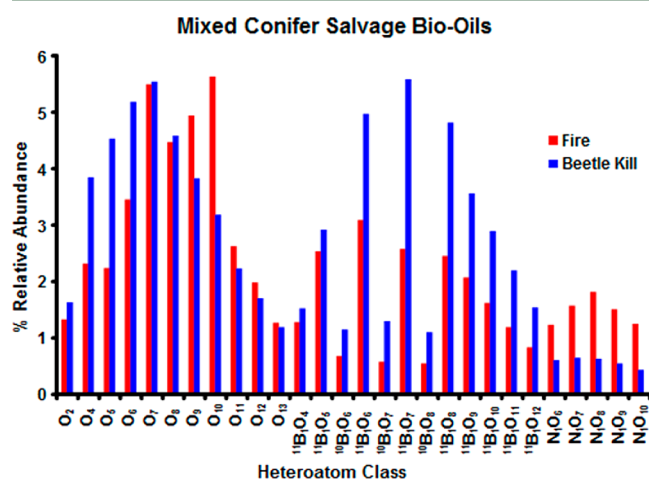

Figure 4. Heteroatom class distribution for the mixed conifer fire (red) and beetle kill (blue) salvage bio-oils derived from (−) ESI 9.4 T FT-ICR mass spectra. The greater compositional complexity of the fire salvage bio-oil relative to the beetle kill salvage bio-oil is evident from the wider range of classes represented. Heteroatom classes with greater than 1% relative abundance in either sample are shown.

abundances. The main differences in O_x species are that the O_3−O_6 species within the mixed conifer beetle kill salvage bio-oil are greater than in the mixed conifer fire salvage bio-oil. Boron-containing classes also exist in mixed conifer salvage bio-oils in high relative abundance. The mixed conifer beetle kill salvage bio-oil contains a greater abundance and range of boron-containing classes ($^{11}B_1O_4$−$^{11}B_1O_{13}$) relative to the mixed conifer fire salvage which only contains $^{11}B_1O_4$−$^{11}B_1O_{11}$ classes in lower abundance. The relative abundances of the $^{10}B_1O_6$−$^{10}B_1O_8$ classes are ~20% of the corresponding ^{11}B-containing classes as expected. However, the mixed conifer fire salvage bio-oil contains higher heteroatom class complexity with several nitrogen-containing compounds (N_1O_5−N_1O_{11}) with >1% relative abundance and over 100 different heteroatom classes identified (Table S1, Supporting Information).

Figure 5 shows mixed conifer salvage bio-oils negative-ion ESI isoabundance-contoured plots of DBE vs carbon number for various O_x heteroatom classes. Both mixed conifer salvage bio-oils have the same compositional space (C# and DBE) coverage for classes O_2 and O_4−O_{13}. The multimodal distributions seen in the oak, scotch broom, and mixed conifer O_x plots (Figure 3) are not seen in either mixed conifer salvage bio-oil in which the dominant distribution covers a narrower range of carbon numbers for a given DBE; thus, mixed conifer salvage bio-oils are less compositionally (C# and DBE) diverse.

Negative-ion isoabundance-contoured plots of DBE vs carbon number for various boron- and nitrogen-containing classes within mixed conifer salvage bio-oils (Figure 6) exhibit similar compositional space coverage as O_x classes (Figure 5). Both data sets exhibit a proportionate increase in aromaticity with carbon addition, characteristic of a polymeric structural motif. The presence of additional heteroatoms (other than C, H, O) does not alter the C# and DBE distribution profile. Again, the assignment of boron-containing compounds is confirmed by overlapping $^{10}B_1O_x$ and $^{11}B_1O_x$ distributions as seen in the mixed conifer beetle kill salvage plots.
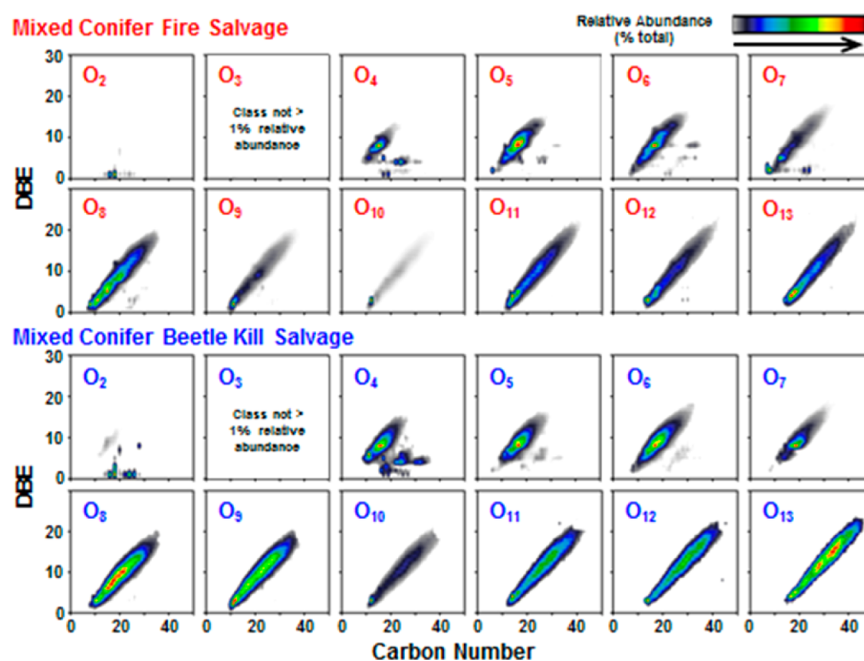
Figure 5. Negative-ion ESI 9.4 T FT-ICR MS isoabundance-contoured double bond equivalents (DBE) vs carbon number plots for the members of the O_2–O_{13} classes from mixed conifer fire (red, top) and beetle kill (blue, bottom) salvage bio-oils. Multimodal compositional distributions found for oak, mixed conifer, and scotch broom bio-oils are not observed for the salvage bio-oils.
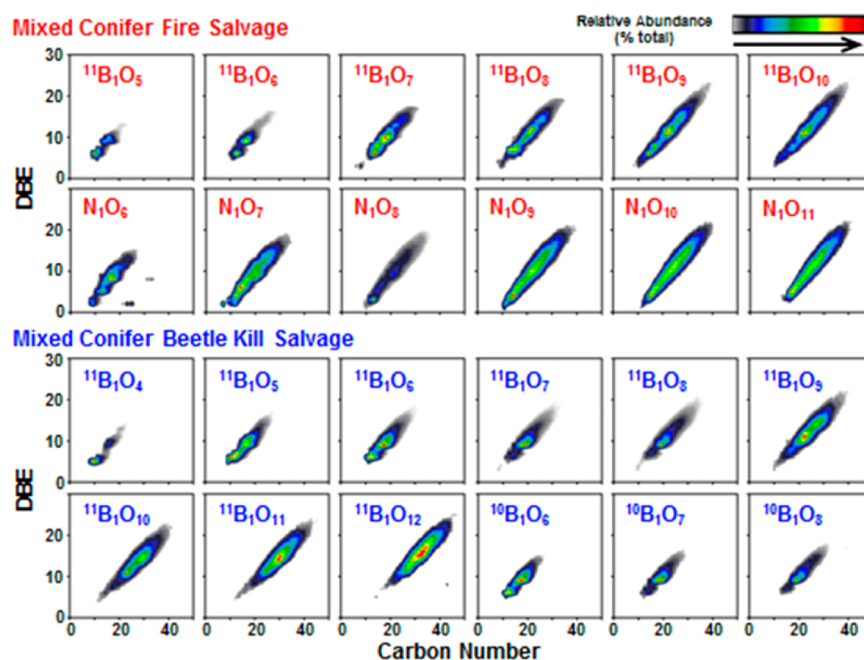

Figure 6. Negative-ion ESI 9.4 T FT-ICR MS isoabundance-contoured double bond equivalents (DBE) vs carbon number plots for the O4 (top) and O6 (bottom) classes from mixed conifer fire (red, top) and beetle kill (blue, bottom) salvage bio-oils. Compounds to the right of the oval have greater alkylation.

Mixed Conifer vs Mixed Conifer Salvage Bio-Oils. A comparison of the compositional space coverage for the mixed conifer and the mixed conifer salvage bio-oils reveals a loss of compositional diversity mostly likely due to differences in feed material (Figure 7). The O_4 and O_6 classes of the mixed conifer bio-oil show a high relative abundance of alkylated compounds (compounds with the same DBE value but an increase in carbon number) whereas the mixed conifer fire salvage bio-oil contains a high relative abundance of highly aromatic core

structures (denoted by red ovals). The mixed conifer beetle kill sample also shows a higher abundance of dealkylated compounds, consistent with the fire salvage bio-oil. Since the same pyrolysis conditions and species of trees (Table 1) were used in all of the mixed conifer feeds, with the an additional species for the beetle kill salvage bio-oil, and we did not see significant compositional (C# and DBE) differences between the two salvage bio-oils, we assume the compositional difference between the mixed conifer and mixed conifer salvage
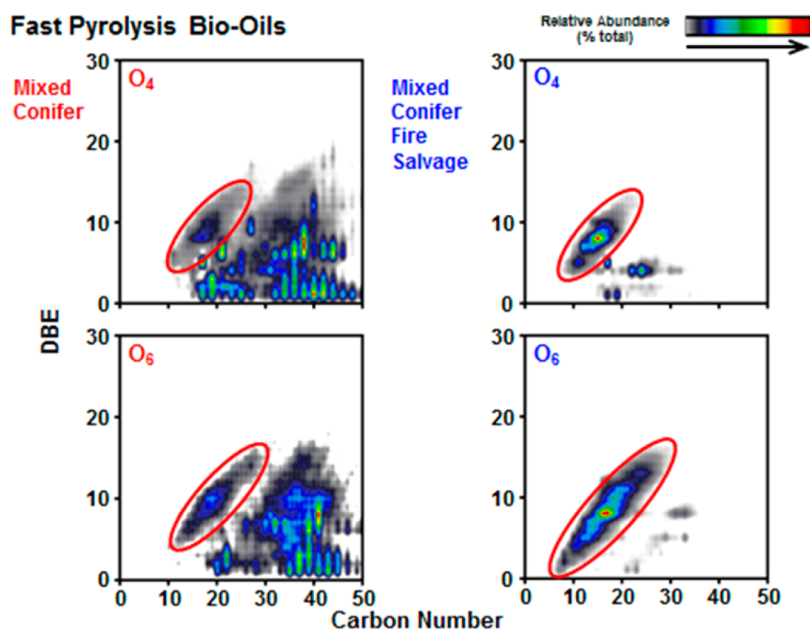
Figure 7. Negative-ion ESI 9.4 T FT-ICR MS isoabundance-contoured double bond equivalents (DBE) vs carbon number plots for the various boron- and nitrogen-containing classes from mixed conifer fire (red, left) and beetle kill (blue, right) salvage bio-oils. The red oval highlights the polycondensed aromatic hydrocarbons (or core structures). As for the O_x classes, data sets exhibit a proportionate increase in aromaticity with carbon addition, characteristic of a polymeric structural motif.
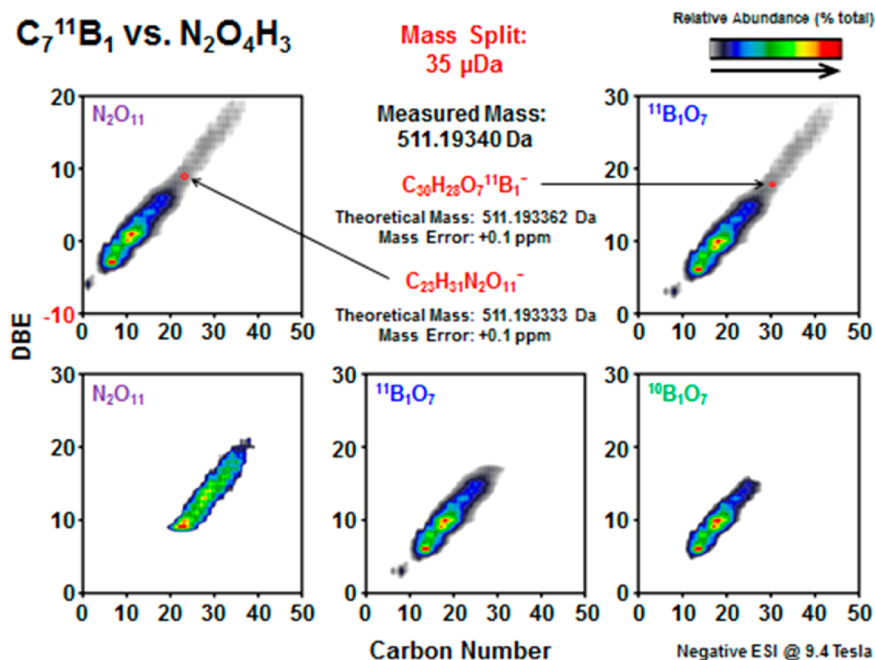

Figure 8. Negative-ion ESI 9.4 T FT-ICR MS isoabundance-contoured double bond equivalent (DBE) vs carbon number plots demonstrating the overlap between boron- and nitrogen-containing compounds from the mixed conifer fire salvage bio-oil. The image at the top left is the result if all the compounds of the Kendrick series are assigned as N_2O_{11} whereas the image at the top right is the result if all the compounds are assigned as $^{11}B_1O_7$. The images on the bottom (N_2O_{11}, left, and $^{11}B_1O_7$, middle) are the way the compounds were assigned on the basis of ^{10}B isotopic verification (right). A single peak at m/z 511.19340 is circled in each of the top images to demonstrate that the peak could correspond to either (or both) a boron- or nitrogen-containing compound based upon mass accuracy.

bio-oils were generated by the conditions that killed the trees (i.e., fire or beetles).

Boron- vs Nitrogen-Containing Compounds. As stated earlier, boron is an essential element for plant development and cell wall structure, so it is not surprising to find boron-containing compounds in bio-oils. Amino acids and alkaloids are known nitrogen-containing compounds present in plants so

their existence in pyrolysis oil is also not unexpected. Since both boron- and nitrogen-containing compounds are inherent to plants, the compounds identified in bio-oils could contain either or both heteroatoms.

Unfortunately, the discovery of boron-containing compounds in bio-oil has significantly complicated accurate molecular formula assignment. There is a 35 μDa mass split

corresponding to the $C_7{}^{11}B_1$ vs $N_2O_4H_3$ mass doublet. Even the best FT-ICR mass spectrometers are not capable of resolving this mass split, so isotopic fine structure is essential to accurately assigning a majority of peaks. Figure 8 depicts the way elemental formulas are assigned to either a nitrogen-containing species or a boron-containing species. From the image at the top left, we see the way the formulas would be assigned if boron was not included in the formula assignment. The image on the top right shows the opposite, if nitrogen was not included and everything was assigned as boron-containing species. From both of these images, we can see that something is possibly misassigned. First off, the image of peaks assigned as N_2O_{11} shows a major part of the distribution below DBE 0, which is not possible. Also, there were some peaks in these Kendrick series that were not even assigned as N_2O_{11} because the carbon number was below 0. This led us to question our original assignments and look for other possible formulas for these compounds. We discovered that there were also Kendrick series of lower abundant peaks 0.996 Da below the peaks assigned to the N_2O_{11} series. The mass difference corresponds with the 0.996 Da mass difference between the isotopes of boron, ^{10}B and ^{11}B. It was determined that the less abundant, lower mass peaks were also ~20% the relative abundance of the more abundant, higher mass peaks. This confirmed our finding that boron-containing species could possibly overlap with nitrogen-containing species.

The next step was to distinguish which peaks belonged to which class. Some classes were easy to separate because there was a jump in DBE, so the lower DBE species were boron-containing species and the higher DBE species were assumed to be nitrogen-containing species. The lower DBE species were confirmed to be boron-containing species with ^{10}B isotopes present whereas the higher DBE species did not have ^{10}B isotopes. However, there were some classes that did not show a jump in DBE. In these cases, the ^{10}B isotopes were used to determine elemental formula assignments (as shown in Figure 8), but there is still a possibility that both species exist and cannot be resolved.

Another issue encountered when assigning boron-containing species is the question of boron's valence. FT-ICR MS cannot determine an element's valence, so an assumption has to be made. For molecular formula assignment and imaging in this manuscript, we assumed the valence of boron is 4 and the negative charge is on the boron since all of the boron-containing compounds identified did not have less than 4 oxygen atoms per molecule, which corresponds with the tetravalent boron complexes previously identified in plants and discussed earlier.[42,43] However, this assumption could be wrong, and the DBE value would be 1 value lower if the valence of boron is 3 and the molecule was deprotonated to result in the negatively charged ion.

Biochar. All biochars produced by fast pyrolysis had approximately the same pH, 7.4 with the mixed conifer fire salvage having the lowest pH (Table 2). However, electrical conductivity (a measure of sample salinity) varied widely; mixed conifer beetle kill salvage had the lowest value (90 μS cm^{-1}), and the mixed conifer fire salvage had the highest (258 μS cm^{-1}). As a comparison, peat moss has an average EC of 4 μS cm^{-1}. Differences in electrical conductivity may be the result of feedstock treatment (e.g., sample drying, conditions of the fire) or the change from *Tsuga heterophylla* in the mixed conifer fire salvage to *Pinus contorta* and *Tsuga mertensiana* in the mixed conifer beetle killed salvage, but this seems unlikely. As

Table 2. Biochar pH and EC from 5 Feedstocks Selected from the Western USA

biochar source	pH	electrical conductivity (μS cm^{-1})
mixed conifer	8.1	103
mixed conifer, fire salvage	7.4	258
mixed conifer, beetle killed	8.1	90
Oregon white oak	7.9	180
scotch broom	7.5	235

expected, all biochar samples consisted of mostly carbon (86–94%).[44] Interestingly, the invasive shrub (scotch broom) had greater quantities of Mg, K, P, S, and Mn than the other biochars. White oak contained the highest levels of Ca. Unlike N, which is volatilized rapidly as temperatures increase,[44] Ca is relatively stable during the pyrolysis process.[45] Calcium, K, Mg, and Fe are the major elements of wood and the subsequent biochars (Table 3). The variability of the biochar produced using a similar pyrolysis machine, but differing feedstocks, points out the need for assessing the location for biochar application, biochar qualities, and the desired soil changes. All biochar will sequester carbon, but the alterations of soil pH and chemical or physical properties should be determined before biochar is applied on a wide scale.[1]

During natural fire events, charcoal (black C) is formed at a rate of about 1–2% of the available biomass.[44] Many forests in the western USA have had fires suppressed for more than 50 years and, therefore, no charcoal added to the soil. Biochar may be one method for increasing forest soil C in these ecosystems.

■ CONCLUSION

Here, we present the detailed characterization of fast pyrolysis bio-oils and biochar generated from various feedstocks by negative-ion ESI FT-ICR MS and other techniques. Oak, mixed conifer, and scotch broom bio-oils exhibit similar compositional (class and space) information which is distinct from mixed conifer salvage bio-oils. The compositional makeup of oak, mixed conifer, and scotch broom bio-oils consists of low O_x species with diverse (several C# for a given DBE) multimodal (O# >2) distributions whereas the mixed conifer salvage bio-oils exhibit a narrow (few C# for a given DBE) monomodal compositional distribution.

Boron-containing classes were also identified in all of the bio-oils analyzed and complicated molecular formula assignment. Since bio-oils have to be upgraded before they can be coprocessed with conventional fuels, it is essential to track the changes in molecular composition as a function of upgrading to determine the viability of the process. Boron- and nitrogen-containing compounds might have huge impacts on the upgrading process. These compounds could potentially cause catalysts poisoning or could be recalcitrant species that resist upgrading treatments. Accurate molecular formula assignment is crucial to understanding what is happening to compounds in bio-oil, and decisions could be made on the basis of inaccurate information if researchers are not aware of the potential for both boron- and nitrogen-containing species to exist.

Ultimately, the fast pyrolysis of forest biomass has the potential to contribute to the world's need for liquid fuels; however, the variability of feedstocks makes it difficult to define the quality of the bio-oil produced. It is also important to note that biochar produced from these western USA feedstocks are also variable. However, this qualitative characterization of bio-

Table 3. Biochar Chemical Composition from 5 Feedstocks from the Western USA

chemical element	mixed conifer	mixed conifer, fire salvage	mixed conifer, beetle killed	Oregon white oak	scotch broom
N (%)	0.26	0.34	0.18	0.62	1.10
C (%)	89	94	86	87	94
Ca (mg mL^{-1})	6700	8700	5100	35000	8000
Mg (mg mL^{-1})	990	1400	930	2300	3100
K (mg mL^{-1})	3900	4600	2400	8600	12000
P (μg g^{-1})	490	730	280	880	1300
S (μg g^{-1})	120	200	120	250	270
Cr (μg g^{-1})	35	61	110	91	46
Cu (μg g^{-1})	12	25	30	40	29
Fe (μg g^{-1})	3900	9700	13000	13000	6000
Mn (μg g^{-1})	150	190	480	560	610
Zn (μg g^{-1})	33	94	86	65	91

oil and biochar byproducts is an important step in developing a wider use of fast pyrolysis in forested ecosystems. The use of a renewable and abundant forest biomass that is annually produced through forest harvest residues or hazard fuel reduction can generate significant quantities of biofuels, reduce wildfire risk, and improve forest health.

ASSOCIATED CONTENT

Supporting Information

Table of the number of peaks assigned to individual heteroatom classes and their corresponding relative abundance derived from (−) 9.4 T ESI FT-ICR mass spectra. This material is available free of charge via the Internet at http://pubs.acs.org.

AUTHOR INFORMATION

Corresponding Author
*E-mail: ddumroese@fs.fed.us.

Author Contributions

The manuscript was written through contributions of all authors. All authors have given approval to the final version of the manuscript.

Notes

The authors declare no competing financial interest.

REFERENCES

(1) McElligott, K.; Page-Dumroese, D.; Coleman, M. *Bioenergy Production Systems and Biochar Application in Forests: Potential for Renewable Energy, Soil Enhancement, and Carbon Sequestration*; U.S. Department of Agriculture, Forest Service, Rocky Mountain Research Station: Fort Collins, 2011.

(2) Rummer, B.; Prestemon, J.; May, D.; Miles, P.; Vissage, J.; McRoberts, R.; Liknes, G.; Shepperd, W. D.; Ferguson, D.; Elliot, W.; Miller, S.; Reutebuch, S.; Barbour, J.; Fried, J.; Stokes, B.; Bilek, E.; Skog, K. *A Strategic Assessment of Forest Biomass and Fuel Reduction Treatments in Western States*; U.S. Dept. of Agriculture, Forest Service, Research and Development: Washington, D.C., 2003.

(3) Badger, P. C.; Fransham, P. Use of Mobile Fast Pyrolysis Plants to Densify Biomass and Reduce Biomass Handling Costs - A Preliminary Assessment. *Biomass Bioenergy* **2006**, *30*, 321−325.

(4) Garcia-Perez, M.; Chaala, A.; Pakdel, H.; Kretchmer, D.; Roy, C. Characterization of Bio-Oils in Chemical Families. *Biomass Bioenergy* **2007**, *31*, 222−242.

(5) Mohan, D.; Pittman, C. U., Jr.; Steele, P. H. Pyrolysis of Wood/Biomass for Bio-Oil: A Critical Review. *Energy Fuels* **2006**, *20*, 848−889.

(6) *Emissions of Greenhouse Gases in the United States 2003*; Technical Report; DOE/EIA-0573 (2003); U.S. Department of Energy: Washington D.C., 2004.

(7) Oasmaa, A.; Kuoppala, E.; Gust, S.; Solantausta, Y. Fast Pyrolysis of Forestry Residue. 1. Effect of Extractives on Phase Separation of Pyrolysis Liquids. *Energy Fuels* **2003**, *17*, 1−12.

(8) Oasmaa, A.; Kuoppala, E.; Solantausta, Y. Fast Pyrolysis of Forestry Residue. 2. Physiochemical Composition of Product Liquid. *Energy Fuels* **2003**, *17*, 433−443.

(9) Oasmaa, A.; Kuoppala, E. Fast Pyrolysis of Forestry Residue. 3. Storage Stability of Liquid Fuels. *Energy Fuels* **2003**, *17*, 1075−1084.

(10) Oasmaa, A.; Kuoppala, E.; Selin, J.-F.; Gust, S.; Solantausta, Y. Fast Pyrolysis of Forestry Residue and Pine. 4. Improvement of Product Quality by Solvent Additive. *Energy Fuels* **2004**, *18*, 1578−1583.

(11) Jarvis, J. M.; McKenna, A. M.; Hilten, R. N.; Das, K. C.; Rodgers, R. P.; Marshall, A. G. Characterization of Pine Pellet and Peanut Hull Pyrolysis Bio-Oils by Negative-Ion Electrospray Ionization Fourier Transform Ion Cyclotron Resonance Mass Spectrometry. *Energy Fuels* **2012**, *26*, 3810−3815.

(12) Smith, E. A.; Park, S.; Klein, A. T.; Lee, Y. J. Bio-Oil Analysis Using Negative Electrospray Ionization: Comparative Study of High Resolution Mass Spectrometry and Phenolics vs. Sugaric Components. *Energy Fuels* **2012**, *26*, 3796−3802.

(13) Liu, Y.; Shi, Q.; Zhang, Y.; He, Y.; Chung, K. H.; Zhao, S.; Xu, C. Characterization of Red Pine Pyrolysis Bio-Oil by Gas Chromatography-Mass Spectrometry and Negative Electrospray Ionization Fourier Transform Ion Cyclotron Resonance Mass Spectrometry. *Energy Fuels* **2012**, *26*, 4532−4539.

(14) Sudasinghe, N.; Dungan, B.; Lammers, P.; Albrecht, K.; Elliott, D.; Hallen, R.; Schaub, T. High Resolution FT-ICR Mass Spectral Analysis of Bio-Oil and Residual Soluble Organics Produced by Hydrothermal Liquifaction of the Marine Microalga *Nannochloropsis salina*. *Fuel* **2014**, *119*, 47−56.

(15) Tessarolo, N. S.; Silva, R. C.; Vanini, G.; Pinho, A.; Romão, W.; de Castro, E. V. R.; Azevedo, D. A. Assessing the Chemical Composition of Biooils using FT-ICR Mass Spectrometry and Comprehensive Two-Dimensional Chromatography with Time-of-Flight Mass Spectrometry. *Microchem. J.* **2014**, *117*, 68−76.

(16) Chiaberge, S.; Leonardis, I.; Fiorani, T.; Cesti, P.; Reale, S.; De Angelis, F. Bio-Oil from Waste: A Comprehensive Analytical Study by

Soft-Ionization FT-ICR Mass Spectrometry. *Energy Fuels* **2014**, *28*, 2019−2026.

(17) Lobodin, V. V.; Nyadong, L.; Ruddy, B. M.; Curtis, M.; Jones, P. R.; Rodgers, R. P.; Marshall, A. G. DART Fourier Transform Ion Cyclotron Resonance Mass Spectrometry for Analysis of Complex Organic Mixtures. *Int. J. Mass Spectrom.***2014**; DOI: 10.1016/j.ijms.2014.07.050.

(18) Dahmen, N.; Henrich, E.; Kruse, A.; Raffelt, K. In *Biomass to Biofuels: Strategies for Global Industries*; Vertès, A. A., Qureshi, N., Blaschek, H. P., Yukawa, H., Eds.; Wiley: West Sussex, U.K., 2010; pp 91−122.

(19) Nelson, D. W.; Sommers, L. E.; Bigham, J. M. In *Methods of Soil Analysis, Part 3 - Chemical Methods*; Sparks, D. L., Page, A. L., Helmke, P. A., Loeppert, R. H., Soltanpour, P. N., Tabatabai, M. A., Johnston, C. T., Sumner, M. E., Eds.; Soil Science Society of America, American Society of Agronomy: Madison, 1996; Vol. *5*, pp 961−1069.

(20) Gavlak, R. G.; Horneck, D. A.; Miller, R. O. *Plant, Soil, and Water Reference Methods for the Western Region*; Western Rural Development Center: Corvallis, 1994; Vol. *125*.

(21) Peech, M. Rapid Microchemical Soil Test. *Soil Sci.* **1944**, *57*, 167.

(22) Murphy, J.; Riley, J. P. A Modified Single Solution Method for the Determination of Phosphate in Natural Waters. *Anal. Chem. Acta* **1962**, *27*, 31−36.

(23) Rhoades, J.D. H. D. Cation Exchange Capacity. In *Methods of Soil Analysis. Part 2*: Chemical and Microbiological Properties; Page, A. L., Ed.; American Society of Agronomy: Madison, 1982; pp 149−157.

(24) Gavlak, R. G.; Horneck, D. A.; Miller, R. O. Western States Laboratory Proficiency Testing Program Soil and Plant Analytical Methods. Version 4.00. In *Plant, Soil, and Water Reference Methods for the Western Region*; Western Rural Development Center: Corvallis, 1997, Vol. *125*, pp 66−67.

(25) Kaiser, N. K.; Quinn, J. P.; Blakney, G. T.; Hendrickson, C. L.; Marshall, A. G. A Novel 9.4 T FTICR Mass Spectrometer with Improved Sensitivity, Mass Resolution, and Mass Range. *J. Am. Soc. Mass Spectrom.* **2011**, *22*, 1343−1351.

(26) Blakney, G. T.; Hendrickson, C. L.; Marshall, A. G. Predator Data Station: A Fast Data Acquisition System for Advanced FT-ICR MS Experiments. *Int. J. Mass Spec.* **2011**, 246−252.

(27) Senko, M. W.; Hendrickson, C. L.; Pasa-Tolic, L.; Marto, J. A.; White, F. M.; Guan, S.; Marshall, A. G. Electrospray Ionization FT-ICR Mass Spectrometry at 9.4 T. *Rapid Commun. Mass Spectrom.* **1996**, *10*, 1824−1828.

(28) Senko, M. W.; Hendrickson, C. L.; Emmett, M. R.; Shi, S. D.-H.; Marshall, A. G. External Accumulation of Ions for Enhanced Electrospray Ionization Fourier Transform Ion Cyclotron Resonance Mass Spectrometry. *J. Am. Soc. Mass Spectrom.* **1997**, *8*, 970−976.

(29) Kaiser, N. K.; Savory, J. J.; McKenna, A. M.; Quinn, J. P.; Hendrickson, C. L.; Marshall, A. G. Electrically Compensated Fourier Transform Ion Cyclotron Resonance Cell for Complex Mixture Mass Analysis. *Anal. Chem.* **2011**, *83*, 6907−6910.

(30) Ledford, E. B., Jr.; Rempel, D. L.; Gross, M. L. Space Charge Effects in Fourier Transform Mass Spectrometry Mass Calibration. *Anal. Chem.* **1984**, *56*, 2744−2748.

(31) Kendrick, E. A Mass Scale Based on CH_2 = 14.0000 for High Resolution Mass Spectrometry of Organic Compounds. *Anal. Chem.* **1963**, *35*, 2146−2154.

(32) Hughey, C. A.; Hendrickson, C. L.; Rodgers, R. P.; Marshall, A. G.; Qian, K. Kendrick Mass Defect Spectroscopy: A Compact Visual Analysis for Ultrahigh-Resolution Broadband Mass Spectra. *Anal. Chem.* **2001**, *73*, 4676−4681.

(33) Warington, K. The Effect of Boric Acid and Borax on the Broad Bean and Certain Other Plants. *Ann. Bot.* **1923**, *37*, 629−672.

(34) Lewis, D. H. Boron, Lignification and the Origin of Vascular Plants-A Unified Hypothesis. *New Phytol.* **1980**, *84*, 209229.

(35) Nielsen, F. H. Boron in Human and Animal Nutrition. *Plant Soil* **1997**, *193*, 199−208.

(36) Benderdour, M.; Bui-Van, T.; Dicko, A.; Belleville, F. *In Vivo* and *In Vitro* Effects of Boron and Boronated Compounds. *J. Trace Elem. Med. Biol.* **1998**, *12*, 2−7.

(37) Goldbach, H. E.; Wimmer, M. A. Boron in Plants and Animals: Is There a Role Beyond Cell-Wall Structure? *J. Plant Nutr. Soil Sci.* **2007**, *170*, 39−48.

(38) Herrera-Rodríguez, M. B.; González-Fontes, A.; Rexach, J.; Camacho-Cristóbal, J. J.; Maldonado, J. M.; Navarro-Gochicoa, M. T. Role of Boron in Vascular Plants and Response Mechanisms to Boron Stresses. *Plant Stress* **2010**, *4*, 115−122.

(39) Kobayashi, M.; Matoh, T.; Azuma, J. I. Two Chains of Rhamnogalacturonan II are Cross-Linked by Borate-Diol Ester Bonds in Higher Plant Cell Walls. *Plant Physiol.* **1996**, *110*, 1017−1020.

(40) Power, P. P.; Woods, W. G. The Chemistry of Boron and Its Speciation in Plants. *Plant Soil* **1997**, *193*, 1−13.

(41) Dembitsky, V. M.; Smoum, R.; Al-Quntar, A. A.; Ali, H. A.; Pergament, I.; Srebnik, M. Natural Occurrence of Boron-Containing Compounds in Plants, Algae and Microorganisms. *Plant Sci.* **2002**, *163*, 931−942.

(42) Matoh, T.; Ishigaki, K.; Ohno, K.; Azuma, J. Isolation and Characterization of a Boron-Polysaccharide Complex from Radish Roots. *Plant Cell Physiol.* **1993**, *34*, 639−642.

(43) Hu, H.; Penn, S. G. C.; Lebrilla, C. B.; Brown, P. H. Isolation and Characterization of Soluble Boron Complexes in Higher Plants-The Mechanism of Phloem Mobility of Boron. *Plant Physiol.* **1997**, *113*, 649−655.

(44) DeLuca, T. H.; Aplet, G. H. Charcoal and Carbon Storage in Forest Soils of the Rocky Mountain West. *Front. Ecol. Environ.* **2008**, *6*, 18−24.

(45) Misra, M. K.; Ragland, K. W.; Baker, A. J. Wood Ash Composition as a Function of Furnace Temperature. *Biomass Bioenergy* **1993**, *4*, 103−116.